Catalysis Today 148 (2009) 36–41

Contents lists available at ScienceDirect

Catalysis Today

journal homepage: www.elsevier.com/locate/cattod

HDS of 4,6-DMDBT over NiW/Al-SBA15 catalysts

Gabriela Macías Esquivel, Jorge Ramírez, Aída Gutiérrez-Alejandre *

UNICAT, Departamento de Ingeniería Química, Facultad de Química, UNAM, Cd. Universitaria, 04510 México D. F., Mexico

ARTICLE INFO

Article history:
Available online 21 May 2009

Keywords:
Al-SBA15
Hydrodesulfurization
NiW catalysts
4,6-DMDBT

ABSTRACT

NiW HDS catalysts supported on alumina-modified SBA-15 were prepared using acidic solutions of ammonium metatungstate and nickel nitrate. Using this method of preparation the integrity of the SBA-15 support was preserved. The results showed that aluminum incorporation into the support framework leads to higher dispersion of the WS_2 phase and gives rise to the formation of Brønsted acid sites, which in turn increase the contribution of the isomerization-direct desulfurization (ISOM-DDS) pathway of 4,6-DMDBT HDS. The higher activity displayed by the Al-modified catalysts in the HDS of 4,6-DMDBT seems to be related to the presence of Brønsted acid sites in the sulfided NiW/Al-SBA15(x) catalysts, to a higher dispersion of the WS_2 phase and to the increased number of coordinatively unsaturated sites (CUS) present in the sulfided catalysts.

1. Introduction

The synthesis of mesoporous silica using triblock copolymer surfactant as templating agent with different ordered porous structures under highly acidic conditions was reported in 1998 by Zhao et al. [1,2]. SBA-15 presents interesting characteristics that make it attractive as support for hydrodesulfurization catalysts. SBA-15 presents adjustable pore size (from 50 to 300 Å), thick pore walls and high hydrothermal stability. The electrically neutral framework of SBA-15 [3–5] can be modified by the incorporation of trivalent heteroatoms such as Al [6,7] either during the synthesis or by post-synthetic methods such as grafting using Al isopropoxide. Incorporation of Al during the synthesis of SBA-15 presents difficulties because under the highly acidic pH needed for the preparation aluminum is dissolved. This problem can be circumvented by introducing aluminum after the synthesis of SBA-15 by grafting either with anhydrous $AlCl_3$ [8], aluminum isopropoxide in non-aqueous solutions [9], or sodium aluminate in aqueous solution [10], followed by calcination.

The incorporation of Al to SBA-15 improves the dispersion of nickel promoted WS_2/SBA-15 HDS catalysts [11]. NiW catalysts supported on different materials have been employed in the hydrodesulfurization of different sulfur molecules with acceptable results [12,13]. It has been reported previously for Mo-based catalysts that aqueous impregnation of AHM (ammonium heptamolybdate) at pH around 5 causes a partial destruction of the SBA-15 ordered porous arrangement [14,15]. However, when AHM is dissolved in a 1:1 demineralized water–chlorhydric acid mixture (pH < 1), the structural integrity of SBA-15 is preserved due to the reaction of the most abundant H_2MoO_4 species with HCl to form MoO_2Cl_2, which does not interact with the silica framework of the mesoporous support [16,17]. For W, at low pH the most abundant species in solution is H_2WO_4 [18]. Therefore, formation of a comparable tungsten precursor is expected in H_2O–HCl solutions. In this case it will be possible to preserve the support hexagonal structural order as it has been reported for NiMo/Al-SBA15(x) catalysts [16].

W-based catalysts are known to have a more hydrogenating character than their Mo counterparts. So, it is interesting to analyze the performance of W-based catalysts, in particular NiW/Al-SBA15 catalysts, during the HDS of 4,6-DMDBT, which goes mainly through a hydrogenation–desulfurization route, the observed trends in hydrogenation will be corroborated by testing the catalysts in the hydrogenation of an aromatic molecule such as naphthalene.

Preservation of the SBA-15 support pore structure during catalyst preparation is of importance to catalyst performance. In this work we will prepare NiW/Al-SBA15(x) catalysts impregnating the Ni and W precursors using HCl acidified solutions. It will be examined if the preparation of the catalyst under acidic conditions preserves the hexagonal arrangement of the Al-SBA15 support. Additionally, the effect of aluminum content on catalyst acidity, dispersion of the active NiW sulfided phase, and preferred reaction routes (HYD or DDS) during the HDS of 4,6-DMDBT, and hydrogenation of naphthalene will be analyzed. Some of the results will be compared with those obtained previously for NiMo/Al-SBA15 catalysts [16].

* Corresponding author. Tel.: +52 55 56225374; fax: +52 55 56225366.
E-mail address: aidag@unam.mx (A. Gutiérrez-Alejandre).

0920-5861/$ – see front matter © 2009 Elsevier B.V. All rights reserved.
doi:10.1016/j.cattod.2009.04.005

2. Experimental

2.1. Support preparation

The synthesis of SBA-15 followed the method outlined by Zhao et al. [1]. For aluminum-modified SBA-15 supports, the required amount of SBA-15 was dispersed in 300 ml of anhydrous hexane (Aldrich 95+%) containing different amounts of aluminum isopropoxide (AIP, Aldrich 98+%) to yield supports with 30 and 15 Si:Al ratio. The resultant mixture was stirred at room temperature during 12 h, and the powder was washed with anhydrous hexane, air dried at room temperature and finally calcined at 823 K during 5 h. The synthesized supports were labeled Al-SBA15(x) where x represents the atomic Si:Al ratio (x = 30, 15).

2.2. NiW catalysts preparation

Ammonium metatungstate (AMT, Fluka $WO_3 \geq 85\%$) was dissolved in a 1:1 demineralized water–concentrated hydrochloric acid (Aldrich 37%) mixture. The Al-SBA15 supports were impregnated by pore volume, dried at 393 K for 12 h and calcined in air at 723 K during 6 h, using a heating ramp of 1 K min^{-1}. In all cases the catalyst loading was 12 wt% WO_3. The Ni promoter was successively impregnated using an aqueous solution of nickel nitrate (Baker 99%) in the required amount to obtain 3 wt% NiO. The catalysts were then dried in air at 393 K for12 h and calcined at 723 K for 4 h (heating rate 1 K min^{-1}).

2.3. Supports and catalysts characterization

The textural properties of supports and catalysts were obtained from nitrogen adsorption–desorption isotherms measured at 77 K with an automatic Micromeritics Tri-Star 3000 analyzer. X-ray diffraction patterns were recorded on a Phillips PW 1050/25 powder diffraction system using Cu Kα radiation with a Ni filter (λ = 1.5406 Å) over the range $3^\circ \leq 2\Theta \leq 90^\circ$ (1° (2Θ) min^{-1}) and $0.5^\circ \leq 2 \leq 8^\circ$ (0.5° (2Θ) min^{-1}). ^{27}Al MAS NMR spectra were recorded on a Bruker Advance 400 equipment, using $Al(H_2O)_6^{3+}$ as external ^{27}Al reference. Determinations were carried out at 300 K with a 104 MHz frequency, a spin rate of 9 kHz and a 0.5 s delayed recycling. FT-Raman spectra were recorded at room temperature on a Nicolet 950 FT-Raman equipped with InGaAs detector and a Nd:YAG laser source with 4 cm^{-1} resolution and 200 scans. For the NO and pyridine adsorption experiments, a thin wafer of the pure catalyst powder was made (8 mg/cm^2) and placed into a special IR cell, then sulfided at the same conditions as for the catalytic test. The sample was then pretreated under vacuum at 773 K for 1 h. After that, a pulse of NO or pyridine was introduced at room temperature and the IR spectra were collected outgassing from room temperature to 373 K. All IR experiments were recorded using a Nicolet IR-Magna 760 spectrometer with 4 cm^{-1} of resolution and 100 scans per spectrum. Sulfided catalysts were characterized by HRTEM using a JEOL 2010 electron microscope with a 1.9-Å point-to-point resolution.

2.4. Catalytic evaluation

Prior to the catalytic test, the oxide catalysts were sulfided ex situ at 673 K during 4 h in 15% H_2S/85% H_2 mixture (25 mL min^{-1}) in a flow reactor. The catalyst was then transferred to the batch reactor under nitrogen atmosphere. The 4,6-DMDBT HDS reaction was performed at 573 K in a Parr batch reactor loaded with 40 ml of a 4,6-DMDBT–decane solution containing the equivalent to 1000 ppm S. After loading the liquid reactants and the catalyst (0.2 g), hydrogen was introduced to the reactor so as to achieve 1000 psia at the reaction temperature. No additional flow of hydrogen was introduced during the reaction.

Naphthalene hydrogenation (HYD) was carried out at 573 K in the same batch reactor, which in this case was loaded with 40 ml of naphthalene–decane solution (25,000 ppm of naphthalene) and 0.2 g of catalyst. The reactor was then pressurized with 600 psia of hydrogen so that at the reaction temperature the pressure was 1000 psia. For catalyst sulfidation and loading of catalyst and reactants the same procedure as for 4,6-DMDBT HDS was used. A sample of the reaction mixture was taken each hour during the 6 h of reaction. Reaction products were analyzed with a HP 6890 Gas Chromatograph equipped with a 50 m length × 0.2 mm diameter × 0.5 μm film thickness capillary column.

3. Results and discussion

3.1. NiW/Al-SBA15(x) catalysts

To analyze the way aluminum interacts with the SBA-15 framework, ^{27}Al MAS NMR spectroscopy experiments were conducted. Fig. 1 shows the ^{27}Al MAS NMR spectra of supports and catalysts.

According to literature the peaks at 50 and 0 ppm are assigned to aluminum in tetrahedral environment (structural unit AlO_4) and to octahedral aluminum (structural unit AlO_6), respectively [19]. The spectra of supports show the presence of AlO_4 and AlO_6 structural units but the intensity of the peaks reveals that aluminum is mainly in tetrahedral coordination, suggesting that most of the grafted aluminum on SBA-15 was incorporated into the silica framework.

When tungsten is impregnated (Fig. 1), the intensity of the peaks localized at 50 and 0 ppm is very similar indicating an increase of octahedral Al species. However, after nickel impregnation, the tetrahedral and octahedral Al peaks in the spectra recover their original proportion. This behavior suggests a strong interaction of W with aluminum, which increases the amount of

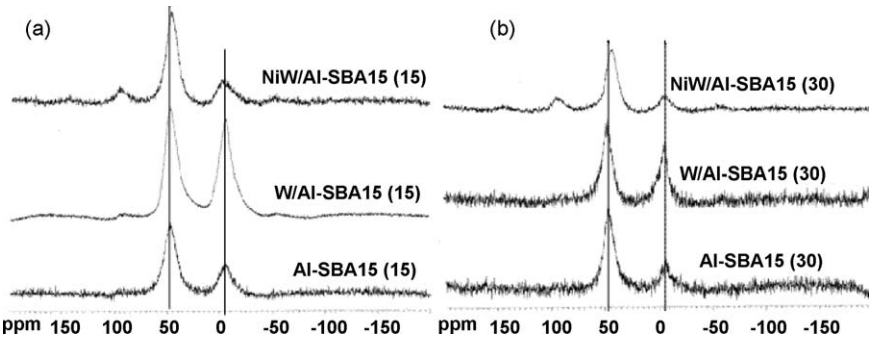

Fig. 1. ^{27}Al MAS NMR spectra of support, W and NiW catalysts supported on (a) Al-SBA-15 (15) and b) Al-SBA-15 (30).

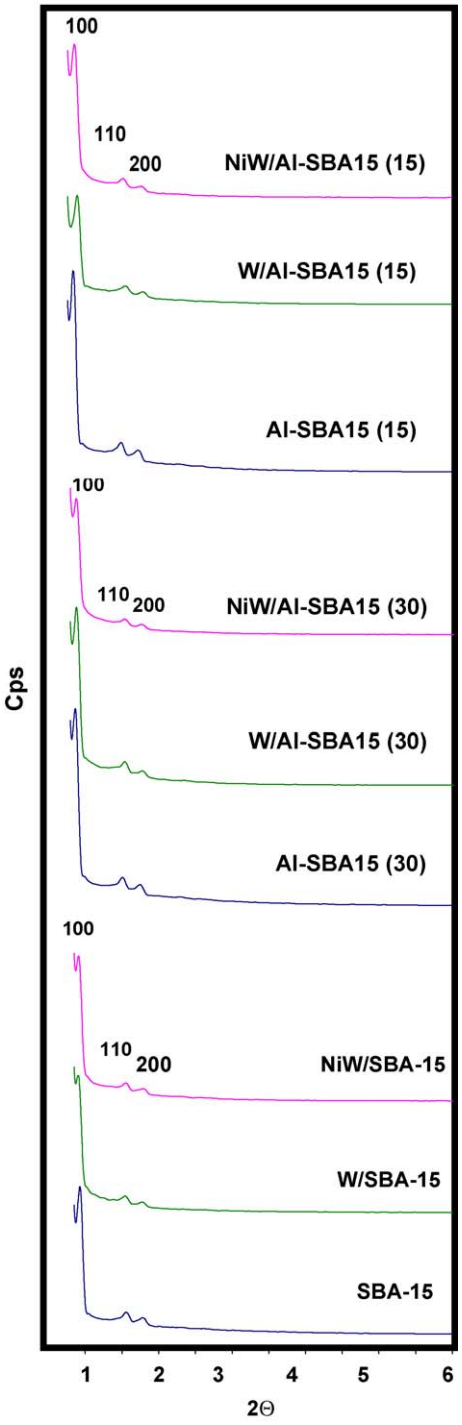

Fig. 2. Diffractograms of catalysts and supports at low angle.

octahedral Al in the sample. However, when Ni is incorporated, the interaction of W with Al diminishes, possibly because the interaction between Ni and W species is favored.

In contrast with the results obtained for Mo-based catalysts [16], tungsten catalysts do not show the presence of a peak at 10 ppm associated to the formation of an hydrated form of aluminum molybdate $Al_2(MoO_4)_3$, possibly an Anderson type heteropolymolybdate $[Al(OH)_6Mo_6O_{18}]^{3-}$.

The diffractograms of all W and NiW catalysts display the three well defined characteristic peaks of SBA-15, indexed as (1 0 0) reflection at 0.93°, (1 1 0) at 1.57° and (2 0 0) at 1.8°, associated with the *p6mm* hexagonal symmetry (Fig. 2). These results indicate

Table 1
Physical properties of supports and NiW catalysts.

	Sg (m^2/g)	$d_{1\,0\,0}$ (Å)	d_{pore} (Å)	a_0 (Å)	E (Å)
SBA-15	903	94.9	65.8	109.6	43.8
Al-SBA-15 (30)	785	95.9	65.6	110.8	45.2
Al-SBA-15 (15)	708	94.9	65.3	109.6	44.3
NiW/SBA-15	617	97.0	65.0	112.0	47.0
NiW/Al-SBA15 (30)	473	94.9	54.6	109.6	55.0
NiW/Al-SBA15 (15)	459	93.9	53.9	108.4	54.5

a_0 = cell parameter, E = wall thickness.

that impregnation of W by the method used here preserves the SBA-15 hexagonal pore structure. After the successive impregnation of Ni the hexagonal structure of SBA-15 was also preserved. This was confirmed by the calculation of the cell parameter a_0 ($a_0 = 2d_{1\,0\,0}/\sqrt{3}$) and $d_{1\,0\,0}$ spacing for all catalysts (Table 1), which are similar to those found in the corresponding supports.

The increase in wall thickness, E ($E = a_0 - d_{pore}$), observed after W and Ni impregnation indicated that the metals are covering the walls of the pores. The diffractograms over the range $3^\circ \leq 2\Theta \leq 90^\circ$ for NiW/Al-SBA15(x) catalysts (Fig. 3), show that only the catalyst supported on pure SBA-15 displays the characteristic reflections associated to WO_3, indicating that tungsten is better dispersed on the aluminum-modified catalysts.

N_2 physisorption isotherms of supports and catalysts (Fig. 4) correspond, according to IUPAC, to a typical irreversible type IV isotherm with H1 hysteresis. The SBA-15 isotherm shows an inflection point at $P/P_0 = 0.6$–0.8, characteristic of capillary condensation inside uniform cylindrical pores. The P/P_0 position of the inflection points corresponds to a pore diameter in the mesoporous range and the sharpness of the step indicates uniformity in the pore size distribution. The increasing shift of the starting point of the hysteresis to lower P/P_0 values with the load of aluminum indicates that alumination of SBA-15 decreases surface area and narrows pore diameter, as Table 1 shows, suggesting the deposition of aluminum on the SBA-15 pore walls.

The form of the isotherms of NiW/Al-SBA15(x) suggests, in agreement with the XRD results, that the structural integrity of SBA-15 remains after nickel and tungsten incorporation.

FT-Raman is a useful technique to observe the structural characteristics of supported oxide species. WO_3 generally gives rise to strong Raman signals whereas those produced by SiO_2 and Al_2O_3 are weak. The characteristic Raman peaks attributed to WO_3 species are located at 811, 717, 605 and 273 cm^{-1} [20]. The FT-Raman spectra of NiW catalysts (not shown), revealed that only the NiW/SBA-15 catalyst presents peaks at 811 and 717 cm^{-1}, associated to WO_3 in agreement with the XRD results.

It is expected that the changes observed in the Ni and W oxide phases with Al incorporation will affect in turn the interaction of Ni and W in the sulfided catalysts. To enquire on this effect, NO

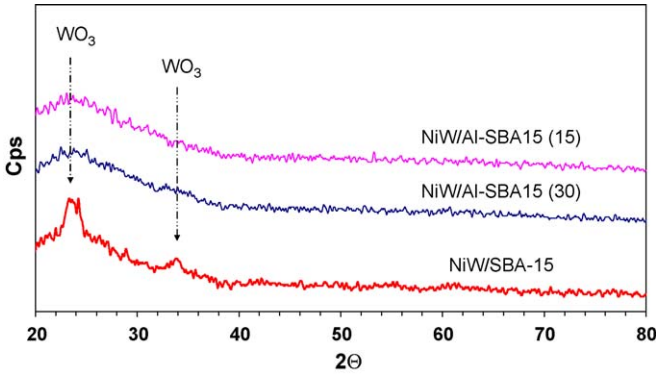

Fig. 3. Diffractograms of catalysts, $3^\circ \leq 2\Theta \leq 90^\circ$.

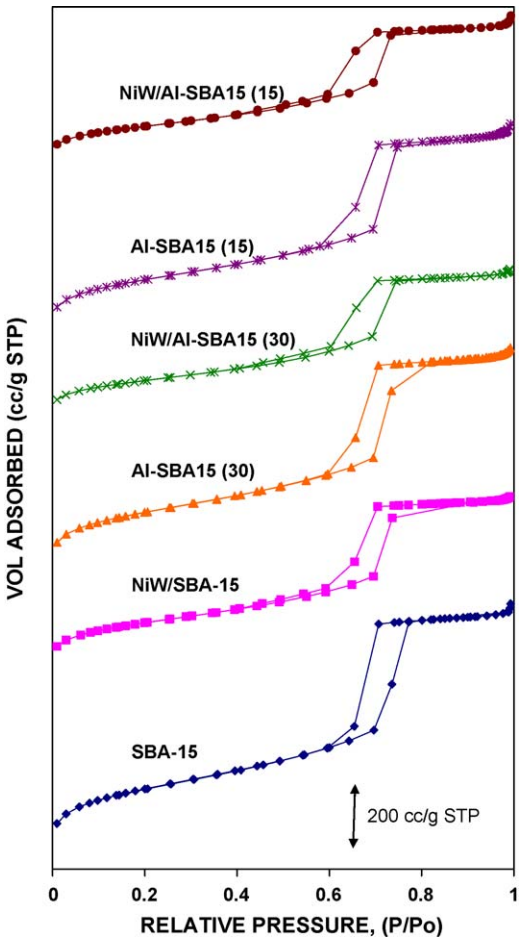

Fig. 4. Nitrogen adsorption–desorption isotherms for supports and NiW catalysts.

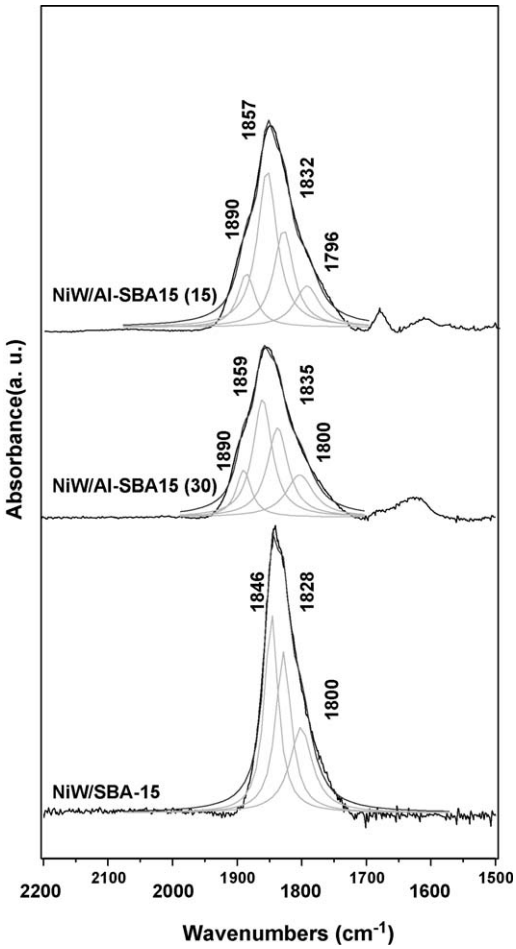

Fig. 5. Deconvolutions of FTIR spectra of adsorbed NO for sulfided NiW/Al-SBA15(x) catalysts.

adsorption experiments were conducted on the different sulfided catalysts. For NiW catalysts, it is reported the existence of four NO infrared bands assigned to adsorbed NO on sulfided Ni^{2+} at 1850 cm^{-1}, sulfided W^{4+} at 1780 cm^{-1}, both sulfided Ni^{2+} and W^{4+} at 1832 cm^{-1}, and Ni^{2+} on oxidic surroundings at 1900 cm^{-1} [21]. NO adsorption FTIR spectra (Fig. 5) show for all NiW/Al-SBA15(x) catalysts a single broad band at 1720-1900 cm^{-1} region, which shifts to 1940 cm^{-1} in the catalysts where the support was modified with aluminum. After a deconvolution process, the presence of bands at 1850, 1832 and 1800 cm^{-1} in every catalyst is evident, but only in those supported on aluminum-modified SBA-15 the band at 1890 cm^{-1} is present. This band is associated to coordinative unsaturated Ni^{2+} species on a different chemical environment due to aluminum interaction with silica. The 1850–1800 cm^{-1} band intensity ratio gives an idea about the proportion of nickel and tungsten coordinatively unsaturated sites (CUS-Ni^{2+}/CUS-W^{4+}) and their value is presented in Table 2. The value of the CUS-Ni^{2+}/CUS-W^{4+} ratio increases with the amount of aluminum incorporated into the support, indicating a higher number of Ni^{2+} CUS sites possibly associated to WS_2 crystallites promoted by nickel, as previously reported [21].

To enquire about the surface acidity of NiW catalysts, pyridine adsorption experiments were conducted. According to literature reports, pyridine adsorbed on Lewis sites gives rise to bands at 1547 and 1640 cm^{-1} and when adsorbed on Brønsted sites there is the presence of bands at 1454 y 1622 cm^{-1}. Bands at 1446 and 1597 cm^{-1} are attributed to hydrogen-bonded pyridine [22]. Fig. 6 shows the IR spectra of NiW catalysts after pyridine adsorption. Only the catalysts supported on Al-modified SBA-15 present Brønsted and Lewis acid sites. It is expected that the presence of Brønsted acid sites will favor the isomerization reaction route of 4,6-DMDBT transformation (see Fig. 7).

HRTEM images (Fig. 8) of sulfided catalysts show the existence of the typical WS_2 layered structures. Over NiW/SBA-15 it is evident that these structures are long and curved and in some cases entangled, while over the aluminum-modified formulations are short and more ordered. This indicates that the aluminum-modified catalysts present higher dispersion of the WS_2 crystallites.

All the above results indicate that Al grafted on the surface of SBA-15 incorporates to the surface mostly as tetrahedral Al

Table 2
Catalytic activity of supported NiW catalysts.

	Xa	k (h^{-1})	HYD/DDS	Tol/MCH	CUS-Ni^{2+}/CUS-W^{4+}	Naphthalene conversion	Type of acidic sites
NiW/SBA-15	0.40	0.141	9.4	1.70	2.30	0.67	Lewis
NiW/Al-SBA15 (30)	0.87	0.389	7.1	1.74	2.80	0.90	Lewis and Brønsted
NiW/Al-SBA15 (15)	0.91	0.407	8	1.84	3.76	0.96	Lewis and Brønsted

Xa = 4,6-DMDBT conversion at t = 6 h, HYD/DDS = hydrogenation products/direct desulfurization product at 35% conversion, Tol/MCH = toluene/methylcyclohexane.

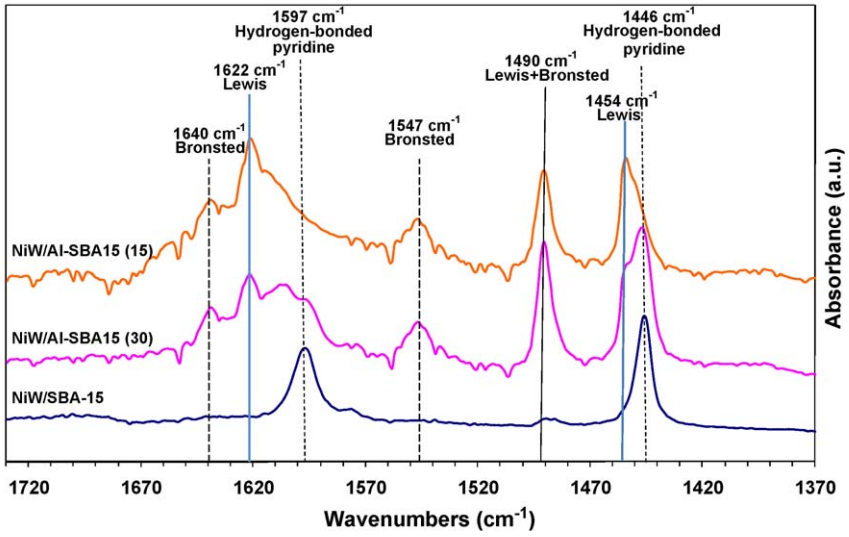

Fig. 6. FTIR spectra of sulfided NiW/SBA-15 and NiW/Al-SBA15(x) catalysts with adsorbed pyridine.

without destroying the SBA-15 porous structure. Impregnation of W and Ni under acidic conditions also preserves the characteristic hexagonal structure of SBA-15. The incorporation of Al to SBA-15 allowed a good dispersion of the W and Ni phases on the surface, which appear to be deposited on the walls of the pores. The increase of the CUS-Ni^{2+}/CUS-W^{4+} ratio indicates that the number of sites associated to the sulfided nickel phase increases with aluminum incorporation to the SBA-15 framework suggesting the formation of more NiWS promoted sites. Also, Brønsted acidic sites, are only present in aluminium-modified SBA-15 supports. So it is possible that the use of these supports favors acid catalyzed reactions like the isomerization contribution during 4,6-DMDBT transformation.

3.2. Catalytic activity

To enquire on the effect of the above changes on the HDS activity, hydrodesulfurization experiments of 4,6-DMDBT were performed. Table 2 shows the HDS conversion results at t = 6 h for 4,6-DMDBT and the values of the pseudo first order reaction rate constant (k, h^{-1}).

Aluminum-modified catalysts present significantly higher HDS activity than the catalyst supported on pure SBA-15. The conversion of 4,6-DMDBT was 91% for NiW/Al-SBA15(15) while only 40% for NiW/SBA-15. The calculated reaction constant values indicate that the catalyst supported on pure SBA-15 displayed an activity 2.28 times smaller than NiW/Al-SBA15 (15).

The reaction pathways for the HDS of 4,6-DMDBT are summarized in Fig. 7. Increasing the acidity of the catalyst can improve its performance due to the displacement of methyl groups (isomerization) induced by the acid character of the catalyst [23–25]. This reduces the sterical hindrance allowing an easier access of the sulfur to the catalyst active site.

Analysis of the reaction pathways was made considering 4,6-dimethyltetrahydrodibenzothiophene (DMTHDBT) and dimethylcyclohexylbenzene (DMCHB) as HYD pathway products, and all dimethylbiphenyls as direct desulfurization (DDS) products. The HYD/DDS and toluene/methylcyclohexane product ratios calculated at 35% 4,6-DMDBT conversions are shown in Table 2. The values of the HYD/DDS ratio are between 7.1 and 9.4, indicating a clear predominance of the hydrogenation route over the hydrodesulfurization one. The incorporation of Al to the catalyst support leads to an increase in HDS activity but also to a decrease in the HYD/DDS ratio. This behavior can be rationalized either by an increase in the DDS routes or a decrease in hydrogenation. Since the contribution of the ISOM-DDS route increases with catalyst acidity, it is possible that the observed decrease in the HYD/DDS ratio is due to a greater relative contribution of the ISOM-DDS pathway. In agreement with this, the value of the Tol/MCH ratio is higher than one for all catalysts and increases from 1.7 to 1.84 with the incorporation of Al. Since the hydrogenation route produces equimolar amounts of toluene and MCH (see Fig. 7), the higher value of the Tol/MCH ratio indicates that other route, most likely the ISOM-DDS one, is producing extra toluene. It has been reported that once 4,6-DMDBT isomerizes the ISOM-DDS route is preferred over the ISOM-HYD pathway [26].

Comparing the results obtained here with those of a previous work on NiMo/Al-SBA-15(x) catalysts [16], it is found that the tungsten-based catalysts of this work present a slightly lower overall HDS activity but higher selectivity towards the hydrogenation route in the transformation of 4,6-DMDBT. For NiMo catalysts the HYD/DDS ratios for the catalysts supported on pure

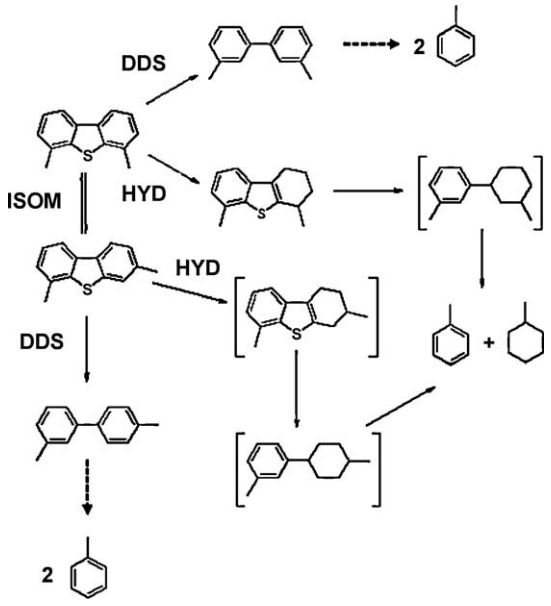

Fig. 7. Scheme for HDS of 4,6-DMDBT through HYD and DDS pathways.

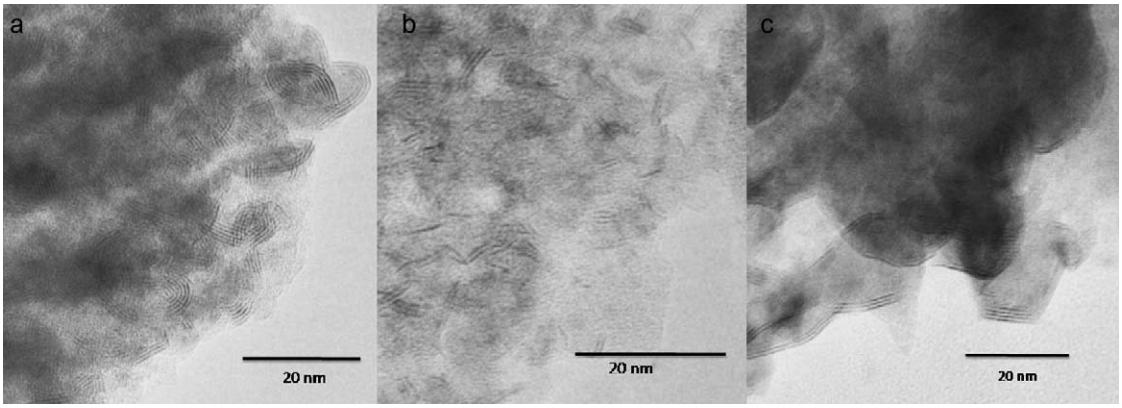

Fig. 8. TEM micrographs of sulfided (a) NiW/SBA-15, (b) NiW/Al-SBA15 (30), and c) NiW/Al-SBA15 (15) catalysts.

SBA-15, Al-SBA15(30), and Al-SBA15(15) were 7.9, 4.5, and 5.1 respectively whereas for the similar W-based catalysts of this work the values of the HYD/DDS ratios were 9.4, 7.1, and 8, respectively. Since in both cases the increase in acidity due to Al incorporation is the same, the results on the HDS of 4,6-DMDBT and particularly the differences in HYD/DDS ratios indicate the more selective hydrogenating character of NiW/Al-SBA15(x) catalysts.

To analyze further the effect that Al incorporation has on the hydrogenating performance of the catalysts, naphthalene hydrogenation was carried out. Conversion of naphthalene after 6 h of reaction is presented in Table 2. NiW/SBA-15 presents the lowest conversion. The HDS activity increases with aluminum content. NiW/Al-SBA15 (30) displayed a conversion 1.3 times higher and NiW/Al-SBA15 (15) 1.4 times that of NiW/SBA-15. So, the use of Al-SBA-15 supports for NiW render HDS catalysts with improved hydrogenation and isomerization functionalities, which are highly active in the hydrodesulfurization of 4,6-DMDBT.

4. Conclusions

When NiW HDS catalysts supported on alumina-modified SBA-15 are prepared using HCl acidified solutions of ammonium metatungstate and nickel nitrate at pH$\sim$1.0 the integrity of the SBA-15 support is preserved. Post-synthetic aluminum incorporation onto the support surface leads to higher dispersion of the WS_2 phase and gives rise to the formation of Brønsted acid sites, which in turn increase the contribution of the isomerization-direct desulfurization (ISOM-DDS) pathway of 4,6-DMDBT HDS. The higher activity displayed by the Al-modified catalysts in the HDS of 4,6-DMDBT seems to be related to the presence of Brønsted acid sites in the sulfided NiW/Al-SBA15(x) catalysts, to a higher dispersion of the WS_2 phase and to the increased number of coordinatively unsaturated sites (CUS) present in the sulfided catalysts. The products distribution shows that the activity of the ISOM-DDS reaction pathway increases with aluminum content, due to the presence of Brønsted acidic sites.

Acknowledgements

Financial support of CONACYT (49479), DGEP, and PAPIIT IN-101406-DGAPA-UNAM programs is acknowledged. We thank Cecilia Salcedo Luna for obtaining XRD patterns, Iván Puente Lee for the TEM work and Gerardo Cedillo Valverde for his help with ^{27}Al MAS NMR experiments.

References

[1] D. Zhao, J. Feng, Q. Huo, N. Melosh, G.H. Fredrickson, B.F. Chmelka, G.D. Stucky, Science 279 (1998) 548.
[2] D. Zhao, Q. Huo, J. Feng, B.F. Chmelka, G.D. Stucky, J. Am. Chem. Soc. 120 (1998) 6024.
[3] R. Mokaya, W. Jones, Chem. Commun. (1997) 2185.
[4] S.K. Jana, T. Kugita, S. Namba, Appl. Catal. A 266 (2004) 245.
[5] R. Mokaya, J. Catal. 193 (2000) 103.
[6] A. Corma, V. Fornés, M.T. Navarro, J. Pérez-Pariente, J. Catal. 148 (1994) 569.
[7] V. Luca, D.J. MacLachlan, R. Bramley, K. Morgan, J. Phys. Chem. 100 (1996) 1793.
[8] R. Ryoo, S. Jun, J.M. Kim, M. Kim, J. Chem. Commun. (1997) 2225.
[9] S.A. Bagshaw, F.D. Renzo, F. Fajula, Chem. Commun. (1996) 2209.
[10] H. Hamdan, S. Endud, H. He, M.N.M. Muhid, J. Klinowski, J. Chem. Soc., Faraday Trans. 92 (1996) 2311.
[11] S. Zeng, J. Blanchard, M. Breysse, Y. Shi, X. Su, H. Nie, D. Li, Appl. Catal. A: Gen. 294 (2005) 59.
[12] J. Ramírez, G. Macías, L. Cedeño, A. Gutiérrez-Alejandre, R. Cuevas, P. Castillo, Catal. Today 98 (2004) 19.
[13] L. Vradman, M.V. Landau, M. Herskowitz, V. Ezersky, M. Talianker, S. Nikitenko, Y. Koltypin, A. Gedanken, J. Catal. 213 (2003) 163.
[14] S.T. Wong, H.P. Lin, C.Y. Mou, Appl. Catal. A 198 (2000) 103.
[15] T. Klimova, E. Rodríguez, M. Martínez, J. Ramírez, Micropor. Mesopor. Mater. 44–45 (2001) 257.
[16] G. Macías, J. Ramírez, A. Gutiérrez-Alejandre, R. Cuevas, Catal. Today 133–135 (2008) 261.
[17] D. Lensveld, Doctoral Thesis, Utrecht University, 2003.
[18] C.F. Baes, R.E. Mesmer, The Hydrolysis of Cations, John Wiley & Sons, New York, 1976, p. 258.
[19] Z. Luan, M. Hartmann, D. Zhao, W. Zhou, L. Kevan, Chem. Mater. 11 (1999) 1621.
[20] L.J. Burcham, I.E. Wachs, Spectrochim. Acta A 54 (1998) 1355.
[21] J. Ramírez, A. Gutiérrez-Alejandre, Catal. Today 43 (1998) 123.
[22] Y. Li, W. Zhang, L. Zhang, Q. Yang, Z. Wei, Z. Feng, C. Li, J. Phys. Chem. B 108 (2004) 9739.
[23] P. Michaud, J.L. Lemberton, G. Pérot, Appl. Catal. A 169 (1998) 343.
[24] T. Isoda, Y. Takase, K. Kusakabe, S. Morooka, Energy Fuels 14 (2000) 585.
[25] E. Lecrenay, K. Sakanishi, I. Mochida, Catal. Today 39 (1997) 13.
[26] G. Pérot, Catal. Today 86 (2003) 111.